

Iridociliary adenocarcinoma with oncocytic change in a dog

Mitsuteru OKAWAUCHI¹⁾, Masaya TSUBOI^{2)*}, Kazumi NIBE^{1, 3)}, Eiji NAGAMINE¹⁾, Hideaki IWANE⁴⁾ and Kazuyuki UCHIDA²⁾

¹⁾Sanritsu Zekkova Veterinary Laboratory, 2–5–8 Kuji, Takatsu-ku, Kawasaki-shi, Kanagawa 213–0032, Japan

²⁾Department of Veterinary Pathology, Graduate School of Agricultural and Life Sciences, The University of Tokyo, 1–1–1 Yayoi, Bunkyo-ku, Tokyo 113–8657, Japan

³⁾Japan Animal Referral Medical Center Kawasaki, 2–5–8 Kuji, Takatsu-ku, Kawasaki-shi, Kanagawa 213–0032, Japan

⁴⁾Iwane Animal Clinic, 468, Murokouji, Takizawa-shi, Iwate 020–0634, Japan

(Received 23 December 2015/Accepted 15 January 2016/Published online in J-STAGE 29 January 2016)

ABSTRACT. An intraocular mass lesion was found in the left eyeball in a spayed female Pembroke Welsh Corgi dog. The surgically resected left eyeball was pathologically examined. Histologically, the mass lesion consisted of proliferation of the atypical cuboidal or columnar epithelial cells, arranging in papillary, tubular or solid form. In addition, some neoplastic cells showed oncocytic change characterized as large oval cells with numerous eosinophilic intracytoplasmic granules. Cytoplasm of the oncocytic cells showed dark blue granules by phosphotungstic acid-hematoxylin stain. Immunohistochemically, the oncocytic cells were intensely positive for cytochrome C. Based on these findings, the ocular mass was diagnosed as iridociliary adenocarcinoma with oncocytic change. The findings indicate that the oncocytic changes of the neoplastic epithelial cells might be caused by mitochondrial accumulation.

KEY WORDS: canine, iridociliary adenocarcinoma, oncocytic change

doi: 10.1292/jvms.15-0721; *J. Vet. Med. Sci.* 78(5): 883–887, 2016

Iridociliary epithelial tumors (ICETs) are neuroectodermal tumors that sporadically occur in the eyes of dogs and cats [7]. In dogs, ICETs are the second most common intraocular neoplasm after the melanocytic tumors, accounting for 12.5% of the total in the Comparative Ocular Pathology Laboratory of Wisconsin (COPLOW) collection [6]. It has been suggested that ICETs are often recognized in middle-aged to old-aged dogs and are more likely to occur in retrievers [7]. In ICETs, the histopathological diagnosis of malignancy is based on anisokaryosis, increased mitotic index and most importantly scleral invasiveness, and the presence of melanin pigment is not related to malignancy [7, 18]. Metastasis of the iridociliary adenocarcinomas is rare, while there was a report concerning lung metastasis [20].

In humans, oncocytomas and/or oncocytic changes have been described in several cases, such as the salivary gland, mammary gland, thyroid and parathyroid glands, adrenal gland, pituitary gland, pancreas, prostate, ovary, kidney, liver, larynx, lung and nasal sinus [1, 2, 10, 15]. Most oncocytic changes are defined as cellular enlargement characterized by abundant granular eosinophilic cytoplasm and mainly regarded as morphological variation reflecting metaplastic change. In dogs, oncocytomas have been reported in the thyroid gland, larynx (rhabdomyoma), kidney and lung

[4, 8, 16, 17], but there is no report in ICETs.

The present report describes histopathological features of iridociliary adenocarcinoma with oncocytic change in a Pembroke Welsh Corgi dog and the immunohistochemical natures of the oncocytic neoplastic cells.

Case history: An uncertain age female spayed Pembroke Welsh Corgi was admitted with decreased visual acuity of the left eye. The intraocular pressure was elevated at 40 mmHg, and a mass lesion was detected in the posterior chamber. The mass appeared brownish, and extended from 9 to 12 o'clock position of the pupillary margin (Fig. 1). The mass size measured by using ultrasound imaging was about 8 mm in diameter. Fifteen days later, the whole left eyeball was surgically enucleated. The dog had histories of malignant melanoma in the right eye and multiple mammary gland tumors including an adenocarcinoma.

Histopathology: The resected tissue was fixed in 10% neutral buffered formalin, processed routinely and embedded in paraffin. Paraffin sections of 4 μ m thick were stained with hematoxylin and eosin (HE), Masson's Trichrome, phosphotungstic acid-hematoxylin (PTAH) and periodic acid-Schiff (PAS). Immunohistochemistry was performed using the Envision polymer system (Dako-Japan, Kyoto, Japan). Table 1 lists the primary antibodies used in this study. The sections were treated with 3% hydrogen peroxide (H₂O₂)-methanol at room temperature for 5 min and incubated in 8% skimmed milk-tris buffered saline (TBS) at 37°C for 40 min to avoid nonspecific reactions. The sections were then incubated at 4°C overnight with primary antibodies. After being washed three times in TBS, the sections were incubated with Envision horseradish peroxidase (HRP) mouse or rabbit polymer (Dako-Japan), or HRP conjugated streptavidin (Dako-Japan) for IgG at room temperature for 40 min. Then, the sections

*CORRESPONDENCE TO: TSUBOI, M., Department of Veterinary Pathology, Graduate School of Agricultural and Life Sciences, The University of Tokyo, 1–1–1, Yayoi, Bunkyo-ku, Tokyo 113–8657, Japan. e-mail: atsuboi@mail.ecc.u-tokyo.ac.jp

©2016 The Japanese Society of Veterinary Science

This is an open-access article distributed under the terms of the Creative Commons Attribution Non-Commercial No Derivatives (by-nc-nd) License <<http://creativecommons.org/licenses/by-nc-nd/4.0/>>.

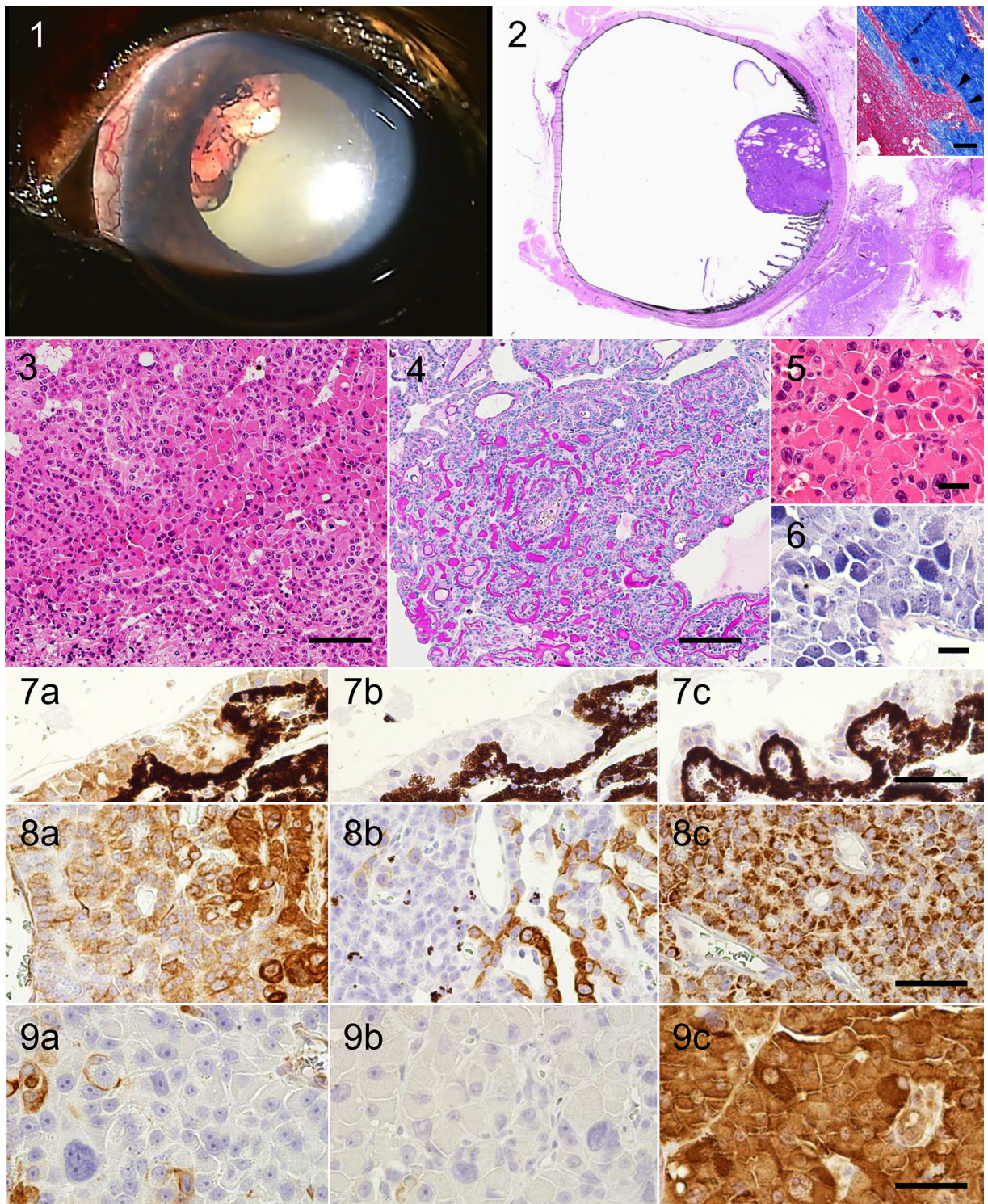


Table 1. Primary antibody used

Antibody	Type (clone)	Clone	Dilution	Source
AE1/AE3	Mouse monoclonal	AE1/AE3	prediluted	Dako, Glostrup, Denmark
CK7	Mouse monoclonal	OV-TL 12/30	1:50	Dako
CK20	Mouse monoclonal	Ks20.8	1:50	Dako
Vimentin	Mouse monoclonal	V9	1:200	Dako
S100	Rabbit polyclonal	-	1:500	Dako
NSE	Rabbit polyclonal	-	prediluted	Nichirei, Tokyo, Japan.
Cytochrome C	Mouse monoclonal	7H8.2C12	1:400	Anaspec, Fremont, U.S.A.
SMA	Mouse monoclonal	1A4	1:100	Dako
Desmin	Mouse monoclonal	D33	1:100	Dako
β III-tubulin	Mouse monoclonal	5G8	1:2,000	Promega, Madison, U.S.A.
Melan A	Mouse monoclonal	A103	1:50	Dako
GFAP	Rabbit polyclonal	-	1:400	Dako

were washed with TBS and visualized with 0.05% 3-3'-diaminobenzidine and 0.01% H₂O₂ in TBS. Counterstaining was performed with Mayer's hematoxylin.

Pathologic findings: The tumor appeared to be derived from the ciliary body epithelium (Fig. 2) and was expanding into the posterior chamber with infiltration into the sclera (Fig. 2, inset). The tumor consisted mainly of nonpigmented epithelium, but sometimes contained a small number of pigmented epithelial cells. The majority of neoplastic cells were cuboidal or columnar form, ranged from solid, papillary to tubular proliferation pattern, had enlarged, variably shaped nuclei with coarse chromatin and sometimes had prominent nucleoli (Fig. 3). Multinucleated cells were occasionally observed. Mitotic figures of the neoplastic cells were 0 to 1 per 10 high power fields. The neoplastic cells were surrounded by PAS-positive, thick-branched basement membranes (Fig. 4). Addition to these findings, oncocytic change was observed in approximately 10% of the neoplastic cells, with oval form with voluminous granular and eosinophilic cytoplasm (Fig. 5). Cytoplasm of the oncocytic cells showed dark blue granules by PTAH stain (Fig. 6).

Immunohistochemical findings: Results of immunohistochemistry against the intact ciliary epithelial cells, cuboidal or columnar neoplastic cells, and oncocytic neoplastic cells are summarized in Table 2.

The intact ciliary epithelial cells were moderately positive for vimentin (Fig. 7a), neuron-specific enolase (NSE) and desmin, and weakly positive for S100. A small number of β III-tubulin-positive cells were scattered in the intact ciliary epithelium. Immunoreactivity for cytokeratin (CK) AE1/AE3 (Fig. 7b), CK20, CK7, glial fibrillary acidic protein (GFAP), smooth muscle actin (SMA) and melan A was not detected. Some epithelial cells showed faint granular cytoplasmic immunoreactivity for cytochrome C (Fig. 7c). On the other hand, almost all cuboidal or columnar neoplastic cells were moderately positive for vimentin (Fig. 8a) and NSE, and were weakly positive for S100. A small number of the cells also had moderate immunoreactivity for AE1/AE3 (Fig. 8b). The neoplastic cells were also moderately positive for cytochrome C (Fig. 8c). The cells were negative for CK20, CK7, GFAP, β III-tubulin, desmin, SMA and melan A. The immunoreactivity of the oncocytic neoplastic

Fig. 1. Gross appearance of the left eye of an uncertain age female spayed Pembroke Welsh Corgi confirmed with iridociliary adenocarcinoma.

The mass appears brownish and extends from 9 to 12 o'clock position of the pupillary margin.

Fig. 2. Low-magnification photomicrograph displaying that the tumor derives from the ciliary body epithelium and is expanding into the posterior chamber. HE. Inset shows that the tumor invades the sclera (upper right, arrowheads). Masson Trichrome. Bar, 100 μ m.

Fig. 3. Photomicrograph of solid or tubular proliferations of neoplastic epithelial cells with enlarged, variably shaped nuclei. Note that subset of neoplastic cells in the center shows oncocytic change. HE. Bar, 100 μ m.

Fig. 4. Photomicrograph of neoplastic cells surrounded by PAS-positive, thick-branched basement membrane material. PAS. Bar, 100 μ m.

Fig. 5. High-magnification photomicrograph of oncocytic neoplastic cells. The enlarged cells are oval formed and have voluminous granular and eosinophilic cytoplasm. HE. Bar, 25 μ m.

Fig. 6. High-magnification photomicrograph of oncocytic neoplastic cells. The cytoplasm of the oncocytic cells shows dark blue granules. PTAH. Bar, 25 μ m.

Fig. 7a-c. Immunohistochemistry of the intact ciliary epithelial cells. (a) Almost all intact ciliary epithelial cells are positive for vimentin. (b) The intact ciliary epithelial cells are negative for AE1/AE3. (c) Some of the intact ciliary epithelial cells are weakly positive for cytochrome C. Bar, 50 μ m.

Fig. 8a-c. Immunohistochemistry of the cuboidal or columnar neoplastic cells. (a) Almost all cuboidal or columnar neoplastic cells are positive for vimentin. (b) A small number of cuboidal or columnar neoplastic cells have moderate immunoreactivity for AE1/AE3. (c) Almost all cuboidal or columnar neoplastic cells are moderately positive for cytochrome C. Bar, 50 μ m.

Fig. 9a-c. Immunohistochemistry of the oncocytic neoplastic cells. (a) The oncocytic neoplastic cells are negative for vimentin. (b) The oncocytic neoplastic cells are negative for AE1/AE3. (c) Almost all oncocytic neoplastic cells are strongly positive for cytochrome C. Bar, 50 μ m.

Table 2. Immunohistochemical reactivity in intact ciliary epithelial cells and ICET cells

Antibody	Intact tissue		Tumor cells			
	Intact ciliary epithelial cells		Cuboidal/columnar cells		Oncocytic cells	
	Positive area	Positive intensity	Positive area	Positive intensity	Positive area	Positive intensity
AE1/AE3	0	-	1	moderate	0	-
CK7	0	-	0	-	0	-
CK20	0	-	0	-	0	-
Vimentin	3	moderate	3	moderate	0	-
Cytochrome C	2	weakly	3	moderate	3	Strongly
Melan A	0	-	0	-	0	-
S100	2	weakly	3	weakly~moderate	3	weakly~moderate
NSE	3	moderate	3	moderate	3	moderate
β III-tubulin	1	moderate	0	-	0	-
GFAP	0	-	0	-	0	-
SMA	0	-	0	-	0	-
Desmin	3	moderate	0	-	0	-

Negative: 0. Positive in 1-25% cells: 1. Positive in 26-50% cells: 2. Positive in more than 51% cells: 3.

cell was almost in conformity with that of cuboidal or columnar neoplastic cells, except for vimentin, AE1/AE3 and cytochrome C. The immunoreactivity of vimentin and AE1/AE3 was not detected in the oncocytic cells (Fig. 9a and 9b). To the contrary, immunoreactivity of cytochrome C was strongly detected and was higher than those of the intact ciliary epithelial and cuboidal or columnar neoplastic cells (Fig. 9c).

Clinical outcome: At the time of two months after surgery, lung metastasis had not been confirmed by chest X-ray. By follow-up phone call at postoperative 13 months, we had confirmed that the patient was alive vigorously.

Histologic features of the tumor of the present case correspond to the previous reports of canine iridociliary adenocarcinoma. The majority of the neoplastic cells were cuboidal to columnar in shape, were proliferating in papillary to tubular pattern and had sclera invasion. Melanoma, medulloepithelioma and other metastatic tumors (such as mammary gland adenocarcinoma) were denied, mainly due to the presence of thick PAS-positive basement membrane and to immunohistochemical profile of the neoplastic cells. Medulloepithelioma, a rare ocular neoplasm in the family of primitive neuroectodermal tumors, is histologically characterized by the presence of tubular rosettes [6, 7]. As the appearance of rosette sometimes resembles tubular pattern, it can be difficult to differentiate from ICETs. As the PAS-positive membranes are frequently observed in ICETs and not in medulloepitheliomas, we excluded the latter. Furthermore, the previous report of immunohistochemical properties of canine ICETs and medulloepitheliomas describes that most iridociliary adenocarcinomas expressed AE1/AE3, while most medulloepitheliomas did not [13]. As a certain number of neoplastic cells in the present case were moderately positive for AE1/AE3, we confirmed the diagnosis as iridociliary adenocarcinoma.

Although the assessment of malignancy is based on its histopathological criteria of scleral invasion and cellular atypia, immunohistochemical profiles of the neoplastic cells

are also coincident with those of the previous malignant ICETs. It seems that the benign iridociliary adenomas are often cytokeratin negative, while its expression appears to increase with increasing aggressiveness of the neoplasm [7, 13]. Klosterman *et al.* observed that CK20 immunostaining was found in most adenomas, while their expression decreases when the tumor acquires aggressiveness [13]. As the neoplastic cells in the present case were positive for AE1/AE3 and negative for CK20, they seem to share the same immunohistochemical profiles as the previous iridociliary adenocarcinomas.

In the present case, some neoplastic cells showed prominent oncocytic change. This change is defined as cellular enlargement characterized by an abundant eosinophilic granular cytoplasm [1]. Oncocytoma, an epithelial tumor that consists of abundant oncocytic change, has been documented in humans, dogs, cats and rats [1-5, 10-12, 15, 16, 19]. In humans, it is seen in many benign and malignant tumors, such as in the salivary gland, mammary gland, thyroid and parathyroid glands, adrenal gland, pituitary gland, pancreas, prostate, ovary, kidney, liver, larynx, lung and nasal sinus [1, 2, 10, 15]. It has been suggested that the oncocytic change is attributed to genetic alterations of mitochondrial DNA and results in cytoplasmic mitochondrial accumulation [1, 9, 15]. Furthermore, the study by Maximo *et al.* describes that Hürthle cells in thyroid carcinoma carries somatic or germline mutations in *GRIM-19* gene (alternative gene symbol known as *NDUFA13*) [14]. The translated protein localizes in the mitochondrial inner membrane and nucleoplasm, and functions as mitochondrial metabolism or cell death regulation. As the oncocytic neoplastic cells in the present case were strongly positive for cytochrome C, a well-known mitochondrial marker [2], it seems that they contain abundant mitochondria in their cytoplasm. This fact indicates that similar mechanism as human oncocytomas might have occurred in the neoplastic cells. Although we wanted to know detailed morphology of the accumulated mitochondria, we could not perform electron microscopy due to lack of tissue samples.

To our knowledge, this is the first report of ICET with oncocytic change in dogs. Although the detailed pathomechanism of this change in canine ICETs still remains unknown, we were able to find a prominent accumulation of mitochondria in the cytoplasm of the oncocytic cells by an immunohistochemical method. Further studies including genetic and morphological analyses are required to investigate into this unique phenomenon.

REFERENCES

1. Asa, S. L. 2004. My approach to oncocytic tumours of the thyroid. *J. Clin. Pathol.* **57**: 225–232. [[Medline](#)] [[CrossRef](#)]
2. Barnes, L. and Bedetti, C. 1984. Oncocytic Schneiderian papilloma: a reappraisal of cylindrical cell papilloma of the sinonasal tract. *Hum. Pathol.* **15**: 344–351. [[Medline](#)] [[CrossRef](#)]
3. Brocks, B. A., Peeters, M. E. and Kimpfler, S. 2008. Oncocytoma in the mandibular salivary gland of a cat. *J. Feline Med. Surg.* **10**: 188–191. [[Medline](#)] [[CrossRef](#)]
4. Buergelt, C. D. and Adjiri-Awere, A. 2000. Bilateral renal oncocytoma in a Greyhound dog. *Vet. Pathol.* **37**: 188–192. [[Medline](#)] [[CrossRef](#)]
5. Doughty, R. W., Brockman, D., Neiger, R. and McKinney, L. 2006. Nasal oncocytoma in a domestic shorthair cat. *Vet. Pathol.* **43**: 751–754. [[Medline](#)] [[CrossRef](#)]
6. Dubielzig, R. R., Ketring, K. L., McLellan, G. J. and Albert, D. M. 2010. The uvea. pp. 245–322. and The Retina. pp. 349–397. *In: Veterinary Ocular Pathology: A Comparative Review*, 1st ed., Saunders, Philadelphia.
7. Dubielzig, R. R., Steinberg, H., Garvin, H., Deehr, A. J. and Fischer, B. 1998. Iridociliary epithelial tumors in 100 dogs and 17 cats: a morphological study. *Vet. Ophthalmol.* **1**: 223–231. [[Medline](#)] [[CrossRef](#)]
8. Dungworth, D. L., Hauser, B., Hahn, F. F., Wilson, D. W., Haenichen, T. and Harkema, J. R. 1999. Tumors of the Larynx and Trachea. pp. 23–25. *In: Histological Classification of Tumors of the Respiratory System of Domestic Animals*, 2nd ser., vol. 6, Armed Force Institute of Pathology and World Health Organization, Washington, D.C.
9. Fusco, A., Viglietto, G. and Santoro, M. 2005. Point mutation in GRIM-19: a new genetic lesion in Hürthle cell thyroid carcinomas. *Br. J. Cancer* **92**: 1817–1818. [[Medline](#)] [[CrossRef](#)]
10. Ghadially, F. N. 1988. *Ultrastructural Pathology of the Cell and Matrix*, 3rd ed., Butterworths, London.
11. Hard, G. C., Seely, J. C. and Betz, L. J. 2014. Spontaneous incidence of oncocytic proliferative lesions in control rat kidney. *Toxicol. Pathol.* **42**: 936–938. [[Medline](#)] [[CrossRef](#)]
12. Kanjo, M., Mitsumori, K., Maita, K. and Shirasu, Y. 1990. Pinnal oncocytoma in a rat. *Vet. Pathol.* **27**: 292–294. [[Medline](#)]
13. Klosterman, E., Colitz, C. M. H., Chandler, H. L., Kusewitt, D. F., Saville, W. J. A. and Dubielzig, R. R. 2006. Immunohistochemical properties of ocular adenomas, adenocarcinomas and medulloepitheliomas. *Vet. Ophthalmol.* **9**: 387–394. [[Medline](#)] [[CrossRef](#)]
14. Máximo, V., Botelho, T., Capela, J., Soares, P., Lima, J., Taveira, A., Amaro, T., Barbosa, A. P., Preto, A., Harach, H. R., Williams, D. and Sobrinho-Simões, M. 2005. Somatic and germline mutation in GRIM-19, a dual function gene involved in mitochondrial metabolism and cell death, is linked to mitochondrion-rich (Hürthle cell) tumours of the thyroid. *Br. J. Cancer* **92**: 1892–1898. [[Medline](#)] [[CrossRef](#)]
15. Mete, O. and Asa, S. L. 2009. Aldosterone-producing adrenal cortical adenoma with oncocytic change and cytoplasmic eosinophilic globular inclusions. *Endocr. Pathol.* **20**: 182–185. [[Medline](#)] [[CrossRef](#)]
16. Meuten, D. J., Calderwood Mays, M. B., Dillman, R. C., Cooper, B. J., Valentine, B. A., Kuhajda, F. P. and Pass, D. A. 1985. Canine laryngeal rhabdomyoma. *Vet. Pathol.* **22**: 533–539. [[Medline](#)] [[CrossRef](#)]
17. Tang, K. N., Mansell, J. L., Herron, A. J. and Sangster, L. T. 1994. The histologic, ultrastructural, and immunohistochemical characteristics of a thyroid oncocytoma in a dog. *Vet. Pathol.* **31**: 269–271. [[Medline](#)] [[CrossRef](#)]
18. Wilcock, B., Dubielzig, R. R. and Render, J. A. 2003. Intraocular Tumors. pp. 22–29. *In: Histological Classification of Ocular and Otic Tumors of Domestic Animals*, 2nd ser., vol. 9, Armed Force Institute of Pathology and World Health Organization, Washington, D.C.
19. You, M. H., Kim, Y. B., Woo, G. H., Kim, J. Y., Yoon, J., Youn, H. Y. and Kim, D. Y. 2011. Nasopharyngeal oncocytoma in a cat. *J. Vet. Diagn. Invest.* **23**: 391–394. [[Medline](#)] [[CrossRef](#)]
20. Zarfoss, M. K. and Dubielzig, R. R. 2007. Metastatic iridociliary adenocarcinoma in a labrador retriever. *Vet. Pathol.* **44**: 672–676. [[Medline](#)] [[CrossRef](#)]